

# Influence of the frameworks of implant-supported prostheses and implant connections on stress distribution

Bruna Santos Honório Tonin<sup>1,B-D</sup>, Raniel Fernandes Peixoto<sup>2,A-C</sup>, Jing Fu<sup>3,C,E</sup>, **Maria da Gloria Chiarello de Mattos**<sup>1,A</sup>, Ana Paula Macedo<sup>1,A-C,F</sup>

<sup>1</sup> Department of Dental Materials and Prosthesis, School of Dentistry of Ribeirão Preto, University of São Paulo, Ribeirão Preto, Brazil

<sup>2</sup> Department of Restorative Dentistry, Faculty of Pharmacy, Dentistry and Nursing, Federal University of Ceará, Fortaleza, Brazil

<sup>3</sup> Department of Prosthodontics, the Affiliated Hospital of Qingdao University, China

A – research concept and design; B – collection and/or assembly of data; C – data analysis and interpretation;

D – writing the article; E – critical revision of the article; F – final approval of the article

Dental and Medical Problems, ISSN 1644-387X (print), ISSN 2300-9020 (online)

*Dent Med Probl.* 2023;60(4):551–557

## Address for correspondence

Bruna Santos Honório Tonin

E-mail: [brunahonin@gmail.com](mailto:brunahonin@gmail.com)

## Funding sources

Grant funding from the São Paulo Research Foundation (FAPESP) (grant No. 2014/11860-3) and Neodent, Curitiba, Brazil (grant No. 208/14).

## Conflict of interest

None declared

## Acknowledgements

None declared

Received on June 27, 2022

Reviewed on July 31, 2022

Accepted on August 29, 2022

Published online on December 15, 2023

## Abstract

**Background.** The maintenance of marginal bone integrity around dental implants continues to be a clinical challenge. It is still unclear whether loading multiple implant-supported prostheses that have different implant connections influences bone resorption.

**Objectives.** The aim of this in vitro study was to compare stress distribution around residual edentulous ridges supported by external hexagon (EH) and Morse taper (MT) implants with screw-retained frameworks obtained with the use of different methods.

**Material and methods.** Three-element implant-supported prostheses with distal cantilevers were manufactured according to different techniques of obtaining the framework: LAS – framework sectioned and welded with a laser; TIG – framework sectioned and welded with tungsten inert gas (TIG); and CCS – framework obtained using a computer-aided design/computer-aided manufacturing (CAD/CAM) system. Occlusal and punctual loading (150 N) was applied to the cantilevers. In the photoelastic stress analysis, the fringe orders ( $n$ ) were quantified using the Tardy method, which calculates the maximum shear stress value ( $\tau$ ) at each selected point.

**Results.** High stress around the implants and tightening were observed in the TIG group, mainly in the crestal bone region for the EH and MT implant connections. The LAS and CCS frameworks exhibited lower stress for the MT connection under occlusal and punctual loading.

**Conclusions.** The comparative analysis of the models showed that the MT connection type associated with the laser-welded or CAD/CAM frameworks resulted in lower stress values in the crestal bone area, suggesting the preservation of bone tissue in this region.

**Keywords:** CAD/CAM, dental prosthesis, dental stress analysis, dental implant

## Cite as

Tonin BSH, Peixoto RF, Fu J, De Mattos MdGC, Macedo AP. Influence of the frameworks of implant-supported prostheses and implant connections on stress distribution. *Dent Med Probl.* 2023;60(4):551–557. doi:10.17219/dmp/153060

## DOI

10.17219/dmp/153060

## Copyright

Copyright by Author(s)

This is an article distributed under the terms of the Creative Commons Attribution 3.0 Unported License (CC BY 3.0) (<https://creativecommons.org/licenses/by/3.0/>).

## Introduction

Residual edentulous ridges may need augmentation procedures before or during implant placement. Some methods are associated with additional surgical intervention, cost, surgical time, and morbidity.<sup>1</sup> Another alternative is rehabilitation with an implant-supported prosthesis with a cantilever. All the force applied in the posterior region of the cantilever is transmitted to the implants, and consequently to the adjacent bone, which causes some concerns regarding stress distribution.<sup>2</sup> Previous studies compared different implant systems in terms of stress distribution with regard to the bone.<sup>3,4</sup> However, these studies used only one element or multiple elements splinted to implant-retained restorations without a cantilever. Thus, research is still required to make this method safer.

To minimize distortion in the framework, and consequently reduce the stress transmitted to the implant-supported system, it is possible to section and weld one-piece frameworks obtained by conventional casting.<sup>5</sup> Different welding techniques can be applied, such as conventional welding, gas-torch brazing, laser welding, and tungsten inert gas (TIG) welding. The TIG method has been associated with good flexural strength, and even with the resistance and adaptation values superior to laser welding for different metal alloys.<sup>6,7</sup> Laser welding has been introduced to dental laboratory procedures as an alternative method to soldering, brazing or TIG welding.<sup>8</sup> Yttrium aluminum garnet (YAG) doped with neodymium (Nd) crystals is used to emit laser beams (the Nd:YAG laser) to weld dental alloys.<sup>9</sup> As the laser energy can be concentrated on a small area, minimal heating or oxidation effects occur in the region surrounding the welded spot; however, this method presents variable resistance results.<sup>10</sup>

Computer-aided design/computer-aided manufacturing (CAD/CAM) can also be used to fabricate implant-supported frameworks.<sup>11,12</sup> This technique has provided significant improvement in the marginal adaption of frameworks,<sup>13</sup> and may result in better stress distribution as compared to frameworks manufactured using traditional laboratory procedures. Although the CAD/CAM technology eliminates several steps, it introduces others, such as scanning, intricate software utilization, design, and machining, which also depend on the experience of the operator and the equipment used.<sup>14</sup>

With regard to the geometry of implant connections, some studies have reported that the Morse taper (MT) connections provide joint stability and higher frictional resistance against rotational and lateral movements under vertical loading than external connections.<sup>15</sup> The external hexagon (EH) connections have been reported to be advantageous in terms of their anti-rotational mechanism and compatibility with different implant systems.<sup>16</sup>

To evaluate biomechanical behavior, photoelasticity has been used. This stress analysis enables the visualization and quantification of stress distribution in its entirety. It shows

how polarized light is affected when passing through a plastic model under experimental loading. The method reveals full-field stress patterns.<sup>17</sup> Photoelastic models have been successfully used to explain differences between various kinds of prosthetic treatment, revealing stress behavior of implant-supported prostheses in the peri-implant bone tissue, and to assess the impact of compromised conditions through comparative stress-related outcome analyses.<sup>17–20</sup> In addition to stress location, its intensity and concentration can be interpreted on the basis of the color, number and closeness of the emerging fringes.<sup>17,21</sup>

The purpose of the present study was to use the photoelastic method to analyze stress distribution around implants supporting a cantilever fixed partial denture (FPD) under both occlusal and punctual loading conditions. The effects of different implant–abutment connections and frameworks, whole and welded, were compared.

## Material and methods

Six photoelastic models were produced from the master polycarbonate models (rectangular block format: 50 mm × 30 mm × 15 mm; 4 mm of height was removed at the posterior region of the model to simulate the resorption of the posterior region of the mandible). The implants (Ø 3.75 mm × 9 mm EH (Ti Titamax; Neodent, Curitiba, Brazil) and Ø 3.75 mm × 9 mm MT (CM Titamax; Neodent)) and a resin tooth were positioned into the models. The implants corresponded to the second premolar and the first molar, and a resin tooth replica (Protemp™ 4; 3M ESPE, St. Paul, USA) replaced the first premolar. The distance between the center of the tooth and the center of the implant was 7.5 mm; the distance between the centers of the implants was 9.5 mm, according to the odontometric parameters described in previous studies.<sup>21–23</sup> The root of the resin tooth received a 0.3-millimeter layer of polyether (Impregum™ Soft; 3M ESPE) to simulate the periodontal ligament (PDL).<sup>24</sup>

A 3-unit implant-retained prosthesis with a distal cantilever was waxed up on the copings of screw-retained abutments (EH and MT abutments, cobalt-chromium (Co-Cr) copings; Neodent). The prosthesis was duplicated (silicone azul; Polglass, Ribeirão Preto, Brazil) to standardize the specimens in all groups. To obtain frameworks, the waxed 3-unit implant-retained prostheses were reduced by 2 mm, and another silicone mold was made. For the fabrication of CAD/CAM frameworks, the previously reduced frameworks were scanned using a D700 scanner (3Shape, Copenhagen, Denmark) and machined in Co-Cr using a milling machine (Ceramill Motion 2; Amman Girrbaach, Koblach, Austria).

The frameworks were fabricated using a Co-Cr alloy (Fit Cast Cobalto; Talmax, Curitiba, Brazil) and separated into the following 3 groups: LAS – conventional cast framework sectioned and welded with a laser; TIG – conventional

cast framework sectioned and welded with TIG; and CCS – framework produced with the CAD/CAM system. Using a 0.5-millimeter-thick, sharp stainless steel blade, the LAS and TIG frameworks were sectioned to be welded after conventional casting. The spruing, investing, burn-out, and casting techniques were standardized. Subsequently, the frameworks were carefully removed by using glass microspheres (Polidental Indústria e Comércio, São Paulo, Brazil) of 100  $\mu\text{m}$  granulation at a pressure of 60 lbf/in<sup>2</sup>. Small nodules were removed with high-speed rotary tungsten carbide burs under constant cooling.

The laser welding machine (desktop Compact; Dentaureum, Nova Lianka, São Paulo, Brazil) was set at 310 V and the pulse was fixed at 9 ms. Laser welding was performed at diametrically opposed points until the entire diameter of the section in the framework received the welding points to minimize distortion. Tungsten inert gas welding was performed using a plasma welding machine (NTY 60 K; Kernit, Indaiatuba, Brazil) according to the adapted methodology.<sup>25</sup> In an argon gas environment, the tungsten (W) electrode was positioned 3–6 mm from the infrastructure, with the settings of 4 A and 0.15 s. Similarly to laser welding, TIG welding was executed at diametrically opposed points on the section of the framework.

All the steps of pressing the infrastructures with the IPS InLine PoM ceramic (Ivoclar Vivadent, Schaan, Liechtenstein) strictly followed the manufacturer's recommendations.

## Photoelastic stress analysis

The abutments were tightened to the implants, and the prosthesis frameworks were tightened on the abutments. Before each analysis, the models were heated to 50°C for 10 min to release the stress induced within the model. Subsequently, the models were cooled at approx. 23°C for 10 min and the absence of residual stresses was confirmed with a polariscope (FL 200; G.U.N.T. Garätebau, Hamburg, Germany).<sup>20</sup> The cantilevers were subjected to a simulated occlusal axial load and a single-point load cell (both of 150 N).<sup>26</sup>

To perform the qualitative analysis, the polariscope was adjusted to the circular polarization mode. Stress intensity, represented by respective fringe orders ( $n$  – number of fringes), and location were compared subjectively. A greater number of fringes indicated greater intensity of tension, and the closer the fringes were to each other, the greater the stress concentration was.<sup>27,28</sup> Interpretation was performed using the following scale: (1) low stress – 1 fringe or less; (2) moderate stress – between 2 and 3 fringes; or (3) high stress – more than 3 fringes.<sup>29</sup>

To perform the quantitative analysis, the polariscope was adjusted to the circular mode. Stress distribution with regard to isochromatic fringes at 6 points of interest (3 in the cervical region of the implants, near the simulated crestal bone, 1 in the apical region of each implant,

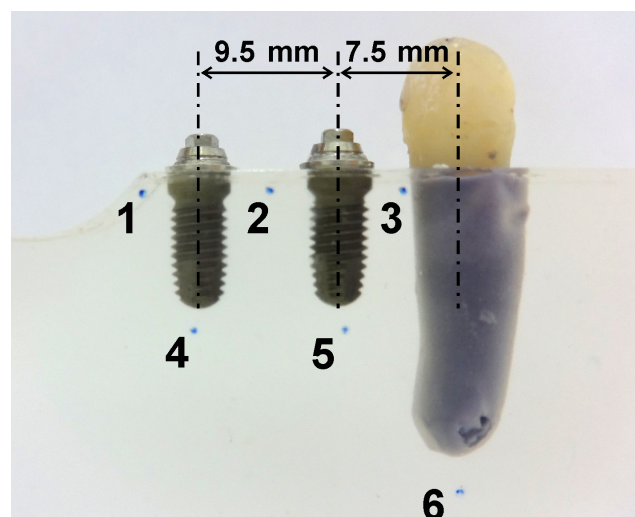


Fig. 1. Distance between the implants and the tooth, and points selected for the quantitative analysis

and 1 in the apical region of the first premolar) (Fig. 1) was analyzed using the photoelastic model. The isochromatic fringe values ( $n$ ) for each of the reading points were measured using the Tardy method of compensation.<sup>30</sup> The individual shear stress value ( $\tau$ ) for each point was determined using the stress-optic law, as follows (Equation 1):

$$\tau = \frac{K_{\sigma} \times n}{2 \times b} \quad (1)$$

where:

$\tau$  – maximum shear stress [kPa];

$n$  – value of the fringe order at the analyzed point; and

$b$  – thickness of the model [mm] (15 mm).

The optical constant of the photoelastic material  $K_{\sigma} = 3.56$  was predetermined in a calibration procedure.<sup>29</sup>

## Results

The photoelastic stress analysis, as showed in Fig. 2 and corroborated by the shear stress values in Table 1, indicated varying stress levels across different scenarios. In the LAS-EH configuration, the observed stress levels were as follows: (1) high between the implants (P2; fringe order 4); (2) moderate between the implant and the tooth (P3, fringe order 2); and (3) moderate in the apical region of the implants (P4 and P5; fringe order 3). The TIG-EH and CCS-EH configurations demonstrated low to moderate stress with a fringe order of 1 at the dental apex (P6) and a fringe order of 2 in the crestal bone region below the cantilever (P1). With regard to the MT connection, TIG-MT exhibited the following stress levels: (1) moderate in the region below the cantilever (P1; fringe order 3); (2) moderate between the implants, and between the implant and the tooth (P2 and P3; fringe order 3); and (3) high in the apical region of the implants



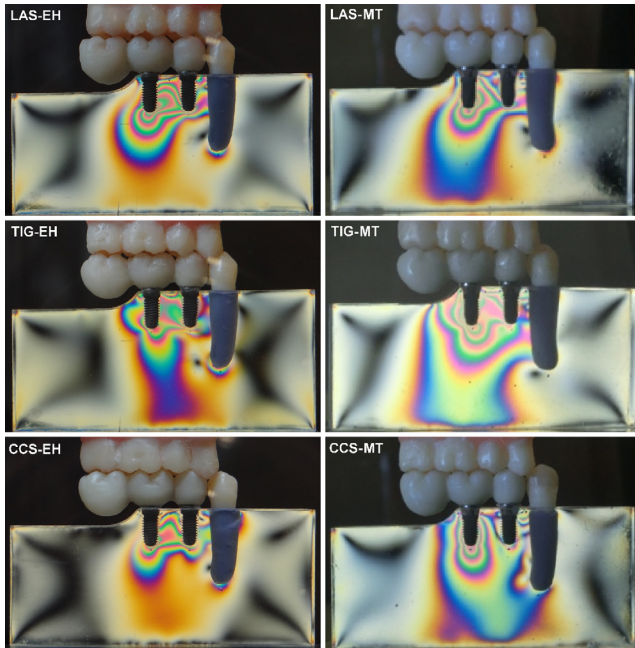


Fig. 2. Stress caused by the application of an occlusal load

LAS – conventional cast framework sectioned and welded with a laser; TIG – conventional cast framework sectioned and welded with tungsten inert gas (TIG); CCS – framework produced with the computer-aided design/computer-aided manufacturing (CAD/CAM) system; EH – external hexagon implant; MT – Morse taper implant.

Table 1. Maximum shear stress values ( $\tau$ ) [kPa] for each point with regard to the external hexagon (EH) and Morse taper (MT) implants under occlusal loading

| Point | EH    |       |       | MT    |       |       |
|-------|-------|-------|-------|-------|-------|-------|
|       | LAS   | TIG   | CCS   | LAS   | TIG   | CCS   |
| P1    | 114.9 | 239.1 | 110.7 | 219.8 | 674.3 | 456.2 |
| P2    | 207.9 | 249.3 | 304.9 | 238.9 | 297.5 | 186.0 |
| P3    | 182.5 | 146.0 | 127.8 | 63.6  | 299.2 | 77.7  |
| P4    | 538.4 | 414.9 | 401.5 | 861.9 | 790.0 | 429.7 |
| P5    | 380.2 | 134.3 | 249.4 | 151.2 | 362.0 | 49.8  |
| P6    | 112.5 | 202.3 | 132.3 | 41.3  | 52.1  | 58.7  |

P1 – below the cantilever; P2 – between the implants; P3 – between the implant and the tooth; P4, P5 – in the apical region of the implants; P6 – at the dental apex.

(P4 and P5, fringe order 4). The LAS-MT and CCS-MT configurations showed fringe order fringe order 1 below the cantilever (P1) and between the implants (P2), and fringe orders 3 and 2 at the apical region of the implants (P4 and P5, respectively).

Regarding the differences in stress distribution between the implant connections under occlusal loading, the LAS-EH configuration exhibited a greater number of fringes between the implants and in the apical regions of the implants. The TIG-MT framework showed the highest stress below the cantilever, in the apical region of the implants, and between the implant and the tooth. Comparing the frameworks fabricated using the CAD/ CAM system, the EH system presented higher stress at all points (except for P1 and P4) as compared to the MT connection.

Under a punctual load of 150 N applied to the cantilever, the photoelastic stress analysis indicated varied stress concentration for the EH and MT implant connections (Fig. 3, Table 2). For the EH connection, the LAS group exhibited a fringe order of 4 at P4, corresponding to a maximum shear stress value of 643.8 kPa. The TIG group showed a fringe order of 3 at points P1, P4, and P5, with notably high shear stress values at P1 (660.7 kPa) and P4 (589.8 kPa). The CCS group demonstrated similar stress patterns, with a fringe order of 3 at P4 and a maximum shear stress value of 637.1 kPa. Other points under the EH connection mostly showed a fringe order of 2, indicating moderate stress levels. For the MT connection, the LAS group presented a high fringe order of 4 at point P4, where the shear stress reached 704.9 kPa. Tungsten inert gas welding on the MT connection produced the highest shear stress across most points, with the peak at P4 (788.4 kPa), followed by P1 (666.9 kPa) and P5 (600.3 kPa). The CCS-MT configuration also showed high stress at P4, with a fringe order of 3 and a shear stress value of 483.4 kPa. Fringe order 2 was observed in the remaining points for all MT groups, suggesting lower stress concentration.

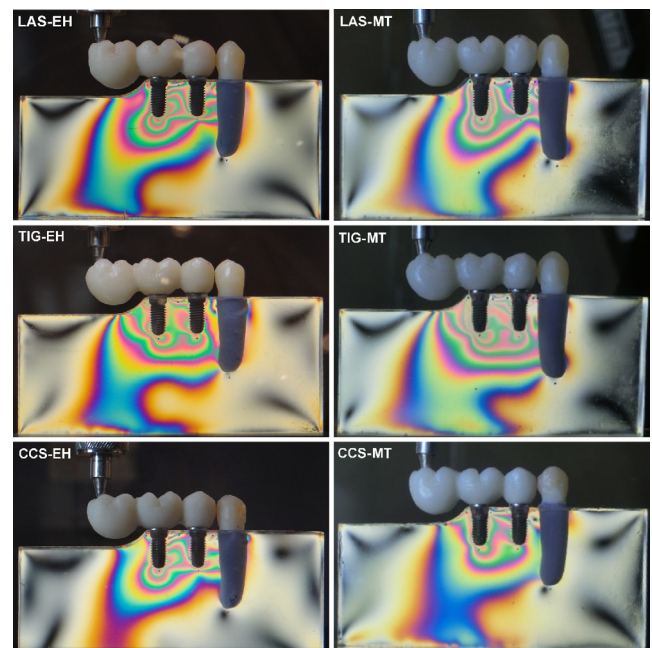


Fig. 3. Stress caused by the application of a punctual load

Table 2. Maximum shear stress values ( $\tau$ ) [kPa] for each point with regard to the external hexagon (EH) and Morse taper (MT) implants under punctual loading

| Point | EH    |       |       | MT    |       |       |
|-------|-------|-------|-------|-------|-------|-------|
|       | LAS   | TIG   | CCS   | LAS   | TIG   | CCS   |
| P1    | 354.0 | 660.7 | 419.1 | 176.8 | 666.9 | 392.5 |
| P2    | 212.9 | 353.8 | 196.9 | 259.3 | 446.3 | 266.5 |
| P3    | 401.3 | 151.3 | 316.0 | 148.8 | 315.7 | 100.0 |
| P4    | 643.8 | 589.8 | 637.1 | 704.9 | 788.4 | 483.4 |
| P5    | 432.6 | 539.9 | 335.4 | 322.3 | 600.3 | 358.7 |
| P6    | 45.6  | 87.9  | 138.6 | 44.6  | 61.2  | 38.8  |

The comparative analysis of the implant connections revealed that the EH system generally exhibited higher shear stress values than the MT connection in certain points within the LAS and CCS groups. Specifically, the LAS-EH configuration showed higher stress at points P1 (354.0 kPa), P3 (401.3 kPa), P5 (432.6 kPa), and P6 (45.6 kPa), while the CCS-EH configuration demonstrated higher values at P1 (419.1 kPa), P3 (316.0 kPa), P4 (637.1 kPa), and P6 (138.6 kPa).

## Discussion

Under occlusal loading, laser welding exhibited the highest stress pattern at the apices of the EH implants, between the implants, and between the implant and the tooth. However, TIG welding presented the highest shear stress in critical areas, such as the crestal bone, for both implant connections. The lost-wax fabrication process of frameworks is related to a high coefficient of thermal expansion of the wax, and its dimensional stability is subject to air temperature; however, a combination of distortions in different dimensions can cause a significant misfit at the prosthesis–abutment interface. Consequently, it may result in the overload of the bone.<sup>31</sup> Although the distortions are difficult to eliminate, they can be minimized by sectioning and welding frameworks.

Laser welding promotes significant mechanical longevity of the framework due to its high precision level, biocompatibility and minimal side effects. Furthermore, this technique yields a framework with reasonable hardness and minimizes the heat-affected zone, which is crucial for maintaining the integrity of the material.<sup>32</sup> De Castro et al. evaluated stress distribution in Co-Cr frameworks with the use of laser welding and TIG welding, and concluded that the stress generated around the implants was similar for both techniques.<sup>25</sup> In the present study, although laser welding presented high stress between the implants, TIG welding showed the highest shear stress values in the crestal bone region at 3 key points, as well as in the apical region of the implants for both the EH and MT connections. This was consistent across all measured points, except for P3 and P4 in the TIG-EH configuration, where the stress was not the highest as compared to other groups, as detailed in Table 2.

In the case of cantilevers, careful planning is necessary to preserve the bone around the implants, mainly because of the distribution of the stress transmitted to the marginal area of the bone during chewing. The concentration of high-intensity fringes at the distal implant under punctual loading on the cantilever, as exhibited by TIG welding in both implant systems, increases the possibility of crestal bone resorption. Some studies have reported an increase in the flexural strength demonstrated by TIG-welded frameworks.<sup>6,7</sup> Several factors may influence the mechanical strength. Tungsten inert gas welding

correlates with resistance because of the welding penetration, consequently resulting in fewer pores, cracks and flaws; thus, high stress to the bone in the crestal bone area can be associated with the high mechanical strength provided by TIG welding.<sup>7</sup>

The study found that the frameworks fabricated using the CAD/CAM technique generally exhibited lower stress values under occlusal and punctual loading. However, this was not consistent across all cases. A detailed examination of Tables 1 and 2 reveals exceptions, where the CAD/CAM frameworks did not result in the lowest stress values as compared to other techniques. Although the CAD/CAM method has improved the fit of frameworks, distortions can still be present when the procedures employed to apply the ceramic involve the lost-wax process followed by heat pressing. Some studies have reported the superiority of the CAD/CAM technique in terms of fit accuracy of implant-supported FDP as compared to the conventional cast frameworks.<sup>11,13</sup> However, these reports compared CAD/CAM with conventional casting, without taking into consideration the copings for the screw-retained abutments, as in the present study. The overcasting technique uses cylinders with pre-machined metal straps to avoid casting the cylinder base and to minimize distortions.<sup>18</sup> This situation may explain the same stress pattern observed for the laser-welded and CAD/CAM frameworks for the MT implants under occlusal and punctual loading on the cantilever.

According to the results, the type of the implant–abutment connection influenced the distribution of stress to the bone. The MT system produced a lower number of fringes and lower shear stress values under both types of loading, except when the framework of the TIG group was tightened. However, a study by Goiato et al. showed a more stable interface for internal connections due to the intimate contact between the internal part of the implant and the external part of the abutment,<sup>33</sup> which favors load distribution.<sup>34</sup> Moreover, the cited study did not use copings for the screw-retained abutments, and only a punctual load was applied to the cantilever. Sousa et al. evaluated the EH and MT connections by using the finite element analysis (FEA), and proved that the MT connection significantly decreased the strain levels in the peri-implant bone.<sup>35</sup> This result is in partial agreement with the findings of the present study, since the TIG group showed the highest shear stress values, especially for the MT connection, which can be attributed to the high flexural strength resulting from the welding penetration.

## Limitations

The photoelastic stress analysis and other *in vitro* methods present certain limitations, and the results should be considered with caution when extrapolating them to clinical situations. These limitations relate to the different elasticity moduli of oral tissues, and the inability of solid,

isotropic photoelastic models to differentiate between the cortical and cancellous bones.<sup>21,36</sup>

Despite the differences, photoelasticity is regarded as a fairly accurate method for assessing stress patterns, as the fundamental stress concentration trends are typically consistent with those observed clinically.<sup>37</sup>

For a more comprehensive understanding, future research could explore three-dimensional (3D) photoelastic stress analysis. This advanced approach would accommodate the complexity of the oral environment more effectively by including shear stress as part of the loading conditions, thereby providing a simulation that would more representative of clinical situations.<sup>19</sup>

## Conclusions

Within the limitations of this study, we conclude that the use of laser-welded and CAD/CAM frameworks with MT implants results in lower stress values in the crestal bone area. Although there was high stress associated with TIG welding on the MT system, the EH system exhibited more stress in other groups in comparison with the MT system.

## Ethics approval and consent to participate

Not applicable.


## Data availability


The datasets generated and/or analyzed during the current study are available from the corresponding author on reasonable request.

## Consent for publication

Not applicable.


## ORCID iDs


Bruna Santos Honório Tonin  <https://orcid.org/0000-0001-7949-9980>

Raniel Fernandes Peixoto  <https://orcid.org/0000-0002-6845-0767>

Jing Fu  <https://orcid.org/0000-0001-6876-6166>

Maria da Gloria Chiarello de Mattos

 <https://orcid.org/0000-0002-1939-7998>

Ana Paula Macedo  <https://orcid.org/0000-0002-7716-106X>

## References

- Ozan O, Kurtulmus-Yilmaz S. Biomechanical comparison of different implant inclinations and cantilever lengths in all-on-4 treatment concept by three-dimensional finite element analysis. *Int J Oral Maxillofac Implants*. 2018;33(1):64–71. doi:10.11607/jomi.6201
- Suedam V, Moretti Neto RT, Capello Sousa EA, Rubo JH. Effect of cantilever length and alloy framework on the stress distribution in peri-implant area of cantilevered implant-supported fixed partial dentures. *J Appl Oral Sci*. 2016;24(2):114–120. doi:10.1590/1678-775720150297
- Pellizzer EP, Carli RI, Falcón-Antenucci RM, Verri FR, Goiato MC, Ribeiro Villa LM. Photoelastic analysis of stress distribution with different implant systems. *J Oral Implantol*. 2014;40(2):117–122. doi:10.1563/AAID-JOI-D-11-00138
- Silveira MPM, Campaner LM, Bottino MA, Nishioka RS, Borges ALS, Tribst JPM. Influence of the dental implant number and load direction on stress distribution in a 3-unit implant-supported fixed dental prosthesis. *Dent Med Probl*. 2021;58(1):69–74. doi:10.17219/dmp/130847
- Matsumoto W, Beraldo PP, De Almeida RP, Macedo AP, Kubata BR, Hotta TH. Evaluation of marginal misfit of metal frameworks welded by gas-torch, laser, and tungsten inert gas methods. *Int J Dent*. 2018;2018:9828929. doi:10.1155/2018/9828929
- Hart CN, Wilson PR. Evaluation of welded titanium joints used with cantilevered implant-supported prostheses. *J Prosthet Dent*. 2006;96(1):25–32. doi:10.1016/j.prosdent.2006.05.003
- Simamoto PC Jr, Novais VR, Machado AR, Soares CJ, Araújo Raposo LH. Effect of joint design and welding type on the flexural strength and weld penetration of Ti-6Al-4V alloy bars. *J Prosthet Dent*. 2015;113(5):467–474. doi:10.1016/j.prosdent.2014.10.010
- Al Jabbari YS, Koutsoukis T, Barmpagadaki X, El-Danaf EA, Fournelle RA, Zinelis S. Effect of Nd:YAG laser parameters on the penetration depth of a representative Ni-Cr dental casting alloy. *Lasers Med Sci*. 2015;30(2):909–914. doi:10.1007/s10103-013-1502-3
- Liu J, Watanabe I, Yoshida K, Atsuta M. Joint strength of laser-welded titanium. *Dent Mater*. 2002;18(2):143–148. doi:10.1016/s0109-5641(01)00033-1
- Lencioni KA, Macedo AP, Silveira Rodrigues RC, Ribeiro RF, Almeida RP. Photoelastic comparison of as-cast and laser-welded implant frameworks. *J Prosthet Dent*. 2015;114(5):652–659. doi:10.1016/j.prosdent.2015.06.005
- De França DG, Morais MH, Das Neves FD, Barbosa GA. Influence of CAD/CAM on the fit accuracy of implant-supported zirconia and cobalt-chromium fixed dental prostheses. *J Prosthet Dent*. 2015;113(1):22–28. doi:10.1016/j.prosdent.2014.07.010
- Tamrakar SK, Mishra SK, Chowdhary R, Rao S. Comparative analysis of stress distribution around CFR-PEEK implants and titanium implants with different prosthetic crowns: A finite element analysis. *Dent Med Probl*. 2021;58(3):359–367. doi:10.17219/dmp/133234
- Da Cunha Fontoura D, De Magalhães Barros V, De Magalhães CS, Vaz RR, Moreira AN. Evaluation of vertical misfit of CAD/CAM implant-supported titanium and zirconia frameworks. *Int J Oral Maxillofac Implants*. 2018;33(5):1027–1032. doi:10.11607/jomi.6320
- Abduo J. Fit of CAD/CAM implant frameworks: A comprehensive review. *J Oral Implantol*. 2014;40(6):758–766. doi:10.1563/AAID-JOI-D-12-00117
- Mangano C, Mangano F, Piattelli A, Iezzi G, Mangano A, La Colla L. Prospective clinical evaluation of 1920 Morse taper connection implants: Results after 4 years of functional loading. *Clin Oral Implants Res*. 2009;20(3):254–261. doi:10.1111/j.1600-0501.2008.01649.x
- Koyama Takahashi JM, Dayrell AC, Xediek Consani RL, De Arruda Nóbilo MA, Pessanha Henriques GE, Mesquita MF. Stress evaluation of implant-abutment connections under different loading conditions: A 3D finite element study. *J Oral Implantol*. 2015;41(2):133–137. doi:10.1563/AAID-JOI-D-11-00205
- Tioosi R, De Torres EM, Rodrigues RC, et al. Comparison of the correlation of photoelasticity and digital imaging to characterize the load transfer of implant-supported restorations. *J Prosthet Dent*. 2014;112(2):276–284. doi:10.1016/j.prosdent.2013.09.029
- Camacho Presotto AG, Brilhante Bhering CL, Mesquita MF, Ricardo Barão VA. Marginal fit and photoelastic stress analysis of CAD-CAM and overcast 3-unit implant-supported frameworks. *J Prosthet Dent*. 2017;117(3):373–379. doi:10.1016/j.prosdent.2016.06.011
- Geramizadeh M, Katoozian H, Amid R, Kadkhodazadeh M. Comparison of finite element results with photoelastic stress analysis around dental implants with different threads. *Dent Med Probl*. 2018;55(1):17–22. doi:10.17219/dmp/85077
- Abarno S, Gehrke AF, Dedavid BA, Gehrke SA. Stress distribution around dental implants, generated by six different ceramic materials for unitary restoration: An experimental photoelastic study. *Dent Med Probl*. 2021;58(4):453–461. doi:10.17219/dmp/135997
- Tonin BSH, Peixoto RF, Fu J, De Freitas BN, De Mattos MdGC, Macedo AP. Evaluation of misfit and stress distribution in implant-retained prosthesis obtained by different methods. *Braz Dent J*. 2021;32(5):67–76. doi:10.1590/0103-6440202104453



22. Otuyemi OD, Noar JH. A comparison of crown size dimensions of the permanent teeth in a Nigerian and a British population. *Eur J Orthod.* 1996;18(6):623–628. doi:10.1093/ejo/18.6.623
23. Bernabé E, Flores-Mir C. Dental morphology and crowding. A multivariate approach. *Angle Orthod.* 2006;76(1):20–25. doi:10.1043/0003-3219(2006)076[0020:DMAC]2.0.CO;2
24. Rabitz GK, Berson R, Caputo AA, Franklin RJ, Del Fierro DB. Load-induced stress in photoelastic primary canines with facial restorations. *J Dent Child (Chic.).* 2006;73(3):170–174. PMID:17367035.
25. De Castro GC, De Araújo CA, Mesquita MF, Xediek Consani RL, De Arruda Nóbilo MA. Stress distribution in Co-Cr implant frameworks after laser or TIG welding. *Braz Dent J.* 2013;24(2):147–151. doi:10.1590/0103-6440201302112
26. De Aguiar FA Jr., Tioosi R, Macedo AP, De Mattos MdAC, Ribeiro RF, Silveira Rodrigues RC. Photoelastic analysis of stresses transmitted by universal cast to long abutment on implant-supported single restorations under static occlusal loads. *J Craniofac Surg.* 2012;23(7 Suppl 1):2019–2023. doi:10.1097/SCS.0b013e3182597c09
27. Machado Nascimento JF, Aguiar-Júnior FA, Nogueira TE, Silveira Rodrigues RC, Leles CR. Photoelastic stress distribution produced by different retention systems for a single-implant mandibular overdenture. *J Prosthodont.* 2015;24(7):538–542. doi:10.1111/jopr.12269
28. Peixoto RF, Tonin BSH, Pinto-Fiamengui LMS, Freitas-Pontes KM, Regis RR, De Mattos MdGC. Analysis of implant-supported cantilever fixed partial denture: An in vitro comparative study on vertical misfit, stress distribution, and cantilever fracture strength. *J Prosthodont.* 2023. doi:10.1111/jopr.13739
29. Akça K, Fanuscu MI, Caputo AA. Effect of compromised cortical bone on implant load distribution. *J Prosthodont.* 2008;17(8):616–620. doi:10.1111/j.1532-849X.2008.00365.x
30. Dally JW, Riley WF, eds. *Experimental Stress Analysis*. 2<sup>nd</sup> ed. New York, NY: McGraw-Hill; 1978.
31. Spazzin AO, Bacchi A, Trevisani A, Farina AP, Dos Santos MB. Fit analysis of different framework fabrication techniques for implant-supported partial prostheses. *Int J Prosthodont.* 2016;29(4):351–353. doi:10.11607/ijp.4542
32. De Luna Gomes JM, De Moraes SL, Araujo Lemos CA, Cruz RS, Oliveira HF, Pellizzer EP. Systematic review and meta-analysis of welding procedures in one-piece cast implant-supported frameworks. *Braz Oral Res.* 2019;33:e110. doi:10.1590/1807-3107bor-2019.vol33.0110
33. Goiato MC, Pesqueira AA, Falcón-Antenucci RM, et al. Stress distribution in implant-supported prosthesis with external and internal implant-abutment connections. *Acta Odontol Scand.* 2013;71(2):283–288. doi:10.3109/00016357.2012.672823
34. Binon PP. Implants and components: Entering the new millennium. *Int J Oral Maxillofac Implants.* 2000;15(1):76–94. PMID:10697942.
35. Sousa RM, Simamoto-Junior PC, Fernandes-Neto AJ, Sloten JV, Jaecques SV, Pessoa RS. Influence of connection types and implant number on the biomechanical behavior of mandibular full-arch rehabilitation. *Int J Oral Maxillofac Implants.* 2016;31(4):750–760. doi:10.11607/jomi.4785
36. Zapparoli D, Peixoto RF, Pupim D, Macedo AP, Toniollo MB, De Mattos MdGC. Photoelastic analysis of mandibular full-arch implant-supported fixed dentures made with different bar materials and manufacturing techniques. *Mater Sci Eng C Mater Biol Appl.* 2017;81:144–147. doi:10.1016/j.msec.2017.07.052
37. Celik G, Uludag B. Photoelastic stress analysis of various retention mechanisms on 3-implant-retained mandibular overdentures. *J Prosthet Dent.* 2007;97(4):229–235. doi:10.1016/j.prosdent.2007.02.006